

An Assessment of How Radiation Incurred During a Mars Mission Could Affect Food and Pharmaceuticals

Myung-Hee Y. Kim and Ianik Plante

Wyle Science, Technology and Engineering Group, Houston, TX 77058

Summary

Radiation levels and associated risks from exposure to galactic cosmic radiation (GCR) during a Mars mission are currently being assessed to protect the health of astronauts. However, the effects of radiation on food and pharmaceuticals that will be stored inside the vehicle during a 3-year journey outside the protection of the geomagnetosphere have yet to be considered. As a first step, we calculated the mean number of charged particle hits and the radiolytic yields in the target materials of freeze-dried food, intermediate moisture food, and liquid formulation pharmaceuticals that are generally considered to be the most vulnerable form of pharmaceuticals. For this assessment the exterior GCR environment at deep solar minimum was assumed to be uniform, isotropic, and constant throughout the entire round-trip journey to Mars. To obtain the total fluence from a 3-year mission, we multiplied the fluence rates by the mission duration. The annual fluence at the target area inside a Mars transfer vehicle was estimated using a sphere of 10 g/cm²-thick aluminum to represent the vehicle. The probability of radiation hits was assessed for a target volume inside the sphere. Additionally, to examine how space radiation may affect taste of food and effectiveness of pharmaceuticals, we simulated yields of the main types of radiolytic species that would be created in liquid water by hits from ions present in GCR. While it is unlikely that GCR causes a rapid change of functional properties in food and pharmaceuticals stored inside the vehicle, it has been suggested that progressive functional defects may occur over time. The functional defects are expected to depend on energy deposition, yields of radiolytic species, bond-dissociation frequency, and any other break-type chemistry. However, the dose received during a 3-year mission to Mars is several orders of magnitude lower than those received for food sterilization or preservation, and the probability of space radiation hitting the individual molecules comprising consumables is very low. In addition it is possible that radiolytic species may not be generated in freeze-dried food or solid formulation drugs because water has been removed during processing. Therefore, space radiation is certainly not a concern for long-term preservation of food or pharmaceuticals. Temperature change, humidity, and packaging technology are much more challenging issues for food preservation or pharmaceutical stability during long duration missions.

1. Dosimetric Quantities and Cancer Risks for Humans from a Mars Mission

Radiation transport through matter was calculated using NASA's theoretical models, specifically the Badhwar-O'Neill 2011 GCR environment model (O'Neill and Foster, 2013) and the high-charge and energy transport (HZETRN) code (Wilson et al., 1994) with the quantum multiple scattering theory of nuclear fragmentation (Cucinotta et

al., 1997). Table 1 shows the annual absorbed dose (D), organ dose (G), and dose equivalent (H) that would be incurred by the charge groups (Z) and the pion and electromagnetic secondaries from exposure to GCR at deep solar minimum (the deepest solar minimum of space era that was recorded in 2009) inside a Mars transfer vehicle. For these calculations a 10 g/cm^2 -thick aluminum sphere was used to represent the vehicle shielding. Table 1 also lists the percent added cancer risk that would be expected from this radiation exposure. Cancer risk values were calculated using the NASA Space Cancer Risk (NSCR-2012) model (Cucinotta et al., 2013). For a 3-year mission with the same continuous GCR fluence rate, the additional cancer risks for astronauts are projected to be 10.98% [2.69%, 26.07%] and 12.38% [2.69%, 27.48%] with the bracketed numbers indicating the 95% confidence intervals for 45-y males and females, respectively. These large risks of cancer induction will surely impose a limit on the number of days astronauts can be exposed to GCR during interplanetary missions. In addition to the health risks imposed from GCR exposure outside the geomagnetosphere, it is necessary to consider any effects on food and pharmaceuticals that will be stored inside the spacecraft for periods that can extend to 3 years for a Mars mission.

2. Atomic Parameters of Target Materials in Food, Water, and Pharmaceuticals

Consumables such as food, water, pharmaceuticals, propellants, and bio-waste products that are stored inside a spacecraft are often proposed as radiation shielding material to protect astronauts on long duration missions. However, food, water, and pharmaceuticals are essential to support life during space travel and one outstanding issue is to ascertain if space radiation poses any harmful effects on the safety and efficacy of these consumables. As a first step in investigating this issue, we assessed the number of ion hits in target sites and the concentrations of radiolytic species induced by space radiation in these consumables. Each type of consumable is defined with specific elemental composition, bulk density, and average molecular weight. Degradation of dietary nutrients or active pharmaceuticals can be addressed by future experimental studies, and these experimental characterizations can then guide the development and validation of simulation models.

Table 2 shows the components of the daily diet recommended for astronauts (AILSS, 1969) including the major chemical formulae of three main macronutrients (carbohydrate, fat, and protein) and the calcium. Oleic fatty acid was used to represent the molecular composition of the total fat in the foods because the most common fats have 16 to 18 carbons (McMurry, 1984) and a large percentage of animal and vegetable fat is composed of oleic fatty acid. The chemical formula for oleic fatty acid is $\text{CH}_3(\text{CH}_2)_7\text{CH}=\text{CH}(\text{CH}_2)_7\text{COOH}$. Carbohydrates comprise simple sugars, such as glucose and fructose. Glucose (from starch and cellulose) and galactose (from gums and fruit pectins) are abundant in nature, and they have the same atomic composition of $\text{CHO}(\text{HOCH})_4\text{CH}_2\text{OH}$ although their molecular structures differ. Amino acids are the building blocks from which all proteins are made. The formulas of twenty common amino acids found in protein (including the 10 essential amino acids that are required in the human diet) have been averaged to obtain the chemical formula, $\text{C}_{5.35}\text{H}_{9.85}\text{O}_{2.35}\text{N}_{1.25}\text{S}_{0.1}$ (McMurry, 1984).

Various types of food are stored onboard a spacecraft including freeze-dried, intermediate moisture, thermo-stabilized, irradiated, natural form, and fresh food. In this present study we considered freeze-dried food and frozen food with intermediate moisture (personal communication with Dr. Lisa Simonsen), two types of food that will be important for longer space missions. Representative atomic parameters of these food types based on the nutrient formula in Table 2 are shown in Tables 3a and 3b for freeze-dried food and frozen food, respectively. Water is an essential life support consumable and also represents the liquid formulation of pharmaceutical drugs. Since it is generally accepted that liquid formulation pharmaceuticals are less stable than solid or semisolid formulations, only liquid formulation is considered in the present manuscript.

3. Mixed-field Radiation inside a Mars Transfer Vehicle

Space radiation includes a large number of particle types and energies from high energy protons to high charge and energy (HZE) particles and they result in a wide range of ionization per track length. Secondary neutrons are also produced from nuclear reactions between the GCR and materials in the spacecraft. Since the composition of the mixed-field radiation is modified when the radiation passes through the vehicle shielding, we estimated the radiation field inside a 10 g/cm²-thick aluminum sphere representing the shielding properties of the vehicle. The annual integral linear energy transfer (LET) distributions of fluence and absorbed dose, shown in Figures 1a and 1b, respectively, represent properties of the simulated GCR exposures to the dried food, frozen food, and water stored in the spacecraft during deep solar minimum conditions. The LET distributions of fluence and absorbed dose are dependent on the atomic parameters of target materials. Further calculations focused on water, because water produces reactive species which can react with molecules in aqueous solution. The differential spectra of particle fluence and absorbed dose in water are shown in Figures 2a and 2b, respectively. These figures show the contributions to particle fluence and dose for each charge group in each energy interval for the mixed-field radiation environments inside a vehicle. Particle fluence and dose peaked around 1,000 MeV/u. Since the fractional contribution of each particle is dependent on the particle type and energy, we restricted our further calculations to the most abundant GCR components for each charge groups, proton ($Z=1$), alpha ($Z=2$), oxygen ($Z=3-9$), and iron ($Z>9$) ions at the energy of 1000 MeV/u.

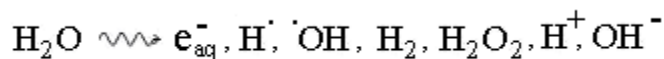
4. Probability of Hits from Mono-Energetic Ions and Estimation of Hit Frequency

To illustrate the microdosimetry properties in water, we calculated the probability of hits for a given absorbed dose of a selected mono-energetic ion using the average-track model (Cucinotta et al., 1998, 2011). The input parameters and the results of the simulation are summarized in Table 4. The total dose of each ion was obtained by multiplying the annual dose of the relevant charge group of GCR and the mission duration (3 years), and the constant particle fluence rates at deep solar minimum were assumed throughout the entire trip. For a given type of radiation (Z and E), the hits by ionizing particles occur randomly along the path of the particle track as it traverses the defined target volume. This is illustrated in Figure 3 as Poisson distribution of the

probability of hits produced inside a $100 \mu\text{m}^2$ area of water from exposure to 0.335 Gy of protons at various energies. Figure 3 displays the probability density of hits from the track core alone, without the contribution of δ -rays, and it shows that the number of ions traversing the target area increases as the proton energy increases. In a living system, the target size is defined as the sensitive site of the system that might be particularly sensitive to the passage of highly ionizing GCR, and it is the important factor for hit analysis using Poisson distribution function as shown in Figure 4. Unlike a living system, all the molecules of consumables are considered equally sensitive and uniformly distributed in the target volume. The volume of the consumable under consideration is represented by a sphere that is calculated using the molecular weight and the specified density of the consumable. For one mole of target material, a large target volume, the number of hits produced along the charged particle path is large and the variation in the number is a small fraction of the total. Therefore, the mean hit frequency of a single molecule can reasonably represent the probability of a molecule being hit by each particle type. Table 5 shows the calculated mean hit frequency for single molecules, including hits by the track core and δ -rays. Since the probability of radiation hits to a molecule is very low, there would be no significant radiation induced alteration to consumables as a result of the accumulated dose from a 3-year mission. However, it is possible that reactive chemical species produced by radiation may damage molecules, or ions in aqueous environments, and this damage could affect the taste or efficacy of food and pharmaceuticals. To examine the properties of chemical reactions, we simulated yields of main radiolytic species induced in water after exposure to various radiation species that comprise GCR.

5. Radiolytic yields

Because food contains some amount of water, the so-called “indirect effects” can be important. Indirect effects involve reaction of chemical species generated by the radiolysis of water with the target molecules. Briefly, irradiation of pure liquid water leads to the formation of radiolytic species, which can be summarized by the following equation:



The most important radiolytic species are $\cdot\text{OH}$, $\text{H}\cdot$, H_2 , H_2O_2 and e_{aq}^- . Some of these radicals react and yield different products. An example of such reaction is:



However, most of them decay to less reactive species in a very short time. For example, the $\cdot\text{OH}$ radical has an in-vivo half-life of $\sim 10^{-9}$ s (Sies, 1993).

The number of species created (or destroyed) is quantified using radiolytic yields which are usually expressed as number of molecules/100 eV of deposited energy. This

can be converted to SI units as 1 molecule/100 eV \approx 0.10364 μ Mol/J. However, reactive species need to be in close proximity for a reaction to occur. In pure liquid water, diffusion can bring reactive species into close proximity within their lifetimes, allowing them to react. In food, especially in frozen foods, it is not clear if such diffusion processes occur. In dehydrated food, many of the radiolytic species may not be created at all.

We have calculated the numbers of molecules \cdot OH, H \cdot , H₂, H₂O₂ and e⁻_{aq} created by the ions, doses and fluences indicated, using the code RITRACKS (Relativistic Ion Tracks), described by Plante and Cucinotta (2011) and references therein. Results are shown in Table 6. The numbers are indicated in nanoMol/L. Although these numbers may appear to be large, the values are accumulated over a 3-year mission and do not take into account the decay of the radiolytic species. Overall, the concentration at any time is very low. This assessment is also a “worst case scenario”, because the calculations are performed for pure water and we don’t expect as many radiolytic species to be formed in food.

A plethora of products, including volatile gas, can be produced during food irradiation (Urbain W, 1986). However, food preservation methods using irradiation are performed with doses in the kGy to MGy range, much higher than the dose for the Mars mission. Many years of scientific evidence have shown that food irradiation is safe. In 1980, the Joint FAO/IAEA/WHO Expert Committee on the Wholesomeness of Irradiated Food (JECFI) declared that “irradiation of any food commodity up to an overall dose of 10 kGy presents no toxicological hazards” (WHO TRS 659, 1981).

6. Concluding Remarks

Food irradiation is not a new subject. As early as in 1905, a British patent was issued for the rights to use ionizing radiation to kill bacteria in foods. A separate U.S. Patent was issued for a preservation technique that combines radioactive material with food (Mollins et al., 2001). In general, food irradiation for sterilization, decontamination and preservation purposes etc. typically uses doses in the kGy range. The radiation dose received during a Mars mission would be several orders of magnitude lower than doses used for food preservation, and our assessment of the numbers of radiation hits and radiolytic species indicates that space radiation would have minor effects on consumables. Radiation is a concern for living organisms because they have critical information, needed for growth and reproduction, encoded in very large molecules. A single change anywhere in this large target can lead to significant harmful effects. This is not the case for food or pharmaceuticals, because they have very large numbers of identical small targets and a significant fraction of them would have to be altered to significantly change the food’s or pharmaceutical’s effectiveness.

Analyses have been performed on a variety of food and pharmaceuticals that were stored on the International Space Station (ISS). The authors of these studies measured the stability of nutrients (Zwart ST et al., 2009) and the physical and chemical changes in pharmaceuticals (Du B et al., 2011) that were stored for up to 880 days on the

ISS and received a radiation exposure of up to 110.7 mGy. The authors concluded that, in general, nutrients and pharmaceuticals in the flight samples did not degrade any faster than the ground controls, and that long-term preservation is more challenging than mitigating the effects of radiation exposure. However, there was a reduction in potency of inflight pharmaceuticals that occurred before the labeled expiration date (Du B et al., 2011). Differences in intact vitamin concentrations due to duration of storage were observed for most foodstuffs (Zwart ST et al., 2009). The most striking changes in nutrients were a 50% decrease in folic acid and thiamin in tortillas, and a 15%-20% decrease in folic acid, vitamin K, and vitamin C in broccoli au gratin. Riboflavin, vitamin A and vitamin C decreased by 10% to 35%. In almonds, hexanal increased by 200% indicating lipid peroxidation, which may affect taste. With regard to taste, anecdotal reports from the astronauts suggest the taste of food changes during spaceflight (Lane et al., 2007). However, taste is largely influenced by smell, which can be affected by odors from different environmental and thermal systems in a spacecraft and compounded by body fluid shifts that cause nasal congestion. Scientists have found that the changes in food created by irradiation are minor compared to those created by cooking. The products created by cooking are so significant that consumers can smell and taste them, whereas detection of low concentration of radiolytic products induced by radiation exposure requires extremely sensitive laboratory equipment.

Acknowledgements

We would like to acknowledge Dr. Walter Schimmerling for his guidance and support in preparing this article, Dr. Sara Zwart at NASA JSC/USRA for useful discussion, and Ms. Kerry George at NASA JSC/Wyle for her thorough review of this manuscript. This work was supported by NASA risk assessment project NAS9-02078.

References

Cucinotta, F. A., Wilson, J. W., and Townsend, L. W. (1997), Abrasion–ablation model for neutron production in heavy ion collisions, *Nucl. Phys. A*, 619, 202–212.

Cucinotta, F. A., Katz, R., and Wilson, J. W. (1998), Radial distribution of electron spectra from high-energy ions, *Radiat. Environ. Biophysics*, 37, 259-265.

Cucinotta, F. A., Kim, M. Y., and Chappell, L. J., Space Radiation Cancer Risk Projections and Uncertainties - 2012, NASA/TP-2013-217375, January 2013.

Cucinotta, F. A., Plante, I., Ponomarev, A. L., and Kim, M. Y. (2011), Nuclear interactions in heavy ion transport and event-based risk models, *Radiat. Prot. Dosimetry*, 143, 384-390.

Du, B., Daniels, V. R., Vaksman, Z., Boyd, J. L., Crady, C., and Putcha, L. (2011), Evaluation of physical and chemical changes in pharmaceuticals flown on space missions, *AAPS J.*, 13(2), June 2011, doi: 10.1208/s12248-011-9270-0.

Hamilton Standard Division, Trade-Off Study and Conceptual Designs of Regenerative Advanced Integrated Life Support Systems (AILSS). Contract No. NAS 1-7905, July 1969.

Lane, H., Zwart, S., Kloeris, V., Smith S. M., and Perchonok M. (2007), Food and nutrition for the moon base, *Nutr. Today*, 42(3), 102-110.

McMurry, J. (1984), *Organic Chemistry*. Brooks/Cole Publishing Company, Monterey, California.

Mollins, R. A. (2001), *Food Irradiation: Principles and Applications*, John Wiley & Sons, New York.

O'Neill, P. M., and Foster, C. C., Badhwar-O'Neill (2011), Galactic Cosmic Ray Flux Model Description, NASA/TP-2013-217376, June 2013.

Plante, I., and Cucinotta, F. A. (2011), in: C.J. Mode (Ed.), *Applications of Monte Carlo Methods in Biology, Medicine and Other Fields of Sciences*, Intech, Rijeka, Croatia, p. 315, doi: 10.5772/15674.

Sies, H. (1993), Strategies of antioxidant defense, *Eur. J. Biochem.*, 215, 213-219.

Urbain, W. R. (1986), *Food Irradiation*, Academic Press, London.

Wilson, J. W., Townsend, L. W., Shinn, J. L., Cucinotta, F. A., Costen, R. C., Badavi, F. F. and Lamkin, S. L. (1994), Galactic cosmic ray transport methods: Past, present, and future, *Adv. Space Res.*, 14, 841–852, doi:10.1016/0273-1177(94)90549-5.

World Health Organization (WHO) (1981), World Health Organization Technical Report Series 659, WHO, Geneva.

Zwart, S. R., Kloeris, V.L., Perchonok, M. H., Braby, L., and Smith, S. M. (2009), Assessment of nutrient stability in foods from the space food system after long-duration spaceflight on the ISS, *J. Food. Sci.*, 74, H209-H217.

Table 1. Simulated annual dosimetric quantities inside a Mars transfer vehicle in the interplanetary space from exposure to GCR at deep solar minimum and the resultant cancer risks for a 45-year old astronaut.

	<i>D</i> , mGy/y	<i>G</i> , mGy-Eq/y	<i>H</i> , mSv/y
Z=1	111.75	167.62	147.06
Z=2	43.58	108.94	173.90
Z=3-9	26.11	65.28	131.75
Z>9	24.66	61.65	432.41
Pion/EM	12.80	15.37	15.37
Total	218.90	418.86	900.49
Cancer risks with 95% CI			
45-y Male	3.80%[0.93%, 8.92%]		
45-y Female	4.35%[0.88%, 10.02%]		

Table 2. Major components of daily diet allowance for astronauts (AILSS, 1969)

	Daily allowance	Chemical formula	MW
Carbohydrates	364 g	$C_6H_{12}O_6$	180 g/Mol
Fat	82 g	$C_{18}H_{34}O_2$	282 g/Mol
Protein	70 g	$C_{5.35}H_{9.85}O_{2.35}N_{1.25}S_{0.1}$	132.35 g/Mol
Calcium	0.8 g	Ca	40 g/Mol
Ascorbic Acid*	70 mg		
Niacin*	17 mg		
Iron*	10 mg		
Total mass	516.8 g		

*Neglected in the current analysis

Table 3a. Atomic parameters for dried food

	Z	A	Atomic Density, atoms/g	MW, g/Mol	ρ , g/cm ³
Carbon	6	12	2.35×10^{22}		
Hydrogen	1	1	4.59×10^{22}		
Oxygen	8	16	1.63×10^{22}	180.6	0.26
Nitrogen	7	14	7.70×10^{20}		
Sulfur	16	32	6.16×10^{19}		
Calcium	20	40	2.33×10^{19}		

Table 3b. Atomic parameters for frozen food (weight fraction of 49.5%/40.5%/10% for food/water/package)

	Z	A	Atomic Density, atoms/g	MW, g/Mol	ρ , g/cm ³
Carbon	6	12	1.65×10^{22}		
Hydrogen	1	1	4.03×10^{22}		
Oxygen	8	16	2.23×10^{22}	30.88	0.414
Nitrogen	7	14	3.94×10^{20}		
Sulfur	16	32	3.15×10^{19}		
Calcium	20	40	1.19×10^{19}		

Table 4. Input parameters and the mean hits on a small target area of water

Input parameters			Atomic interaction output results			
Ions at 1 GeV/u	<i>D</i> , Gy	Target area, μm^2	Fluence, $1/\mu\text{m}^2$	<i>L</i> , keV/ μm	Mean number of hits per 100 μm^2	
					Track core only	With δ - rays (> 1 mGy)
p	0.335	100	9.40	0.22	939.75	1100.22
α	0.131		0.919	0.89	91.87	124.48
^{16}O	0.078		3.42×10^{-2}	14.24	3.42	9.38
^{56}Fe	0.074		3.07×10^{-3}	150.42	0.31	3.01

Table 5. Probability of a molecule being hit (for the calculations the molecule is represented by a sphere)

Ions at 1 GeV/u	<i>D</i> , Gy	Material	Mean hit frequency per mole	Mean hit frequency of a molecule
p	0.335	Dried food	9.18×10^{10}	1.52×10^{-13}
		Frozen food	2.10×10^{10}	3.49×10^{-14}
		Water	7.80×10^9	1.30×10^{-14}
α	0.131	Dried food	8.97×10^9	1.49×10^{-14}
		Frozen food	2.06×10^9	3.41×10^{-15}
		Water	7.63×10^8	1.27×10^{-15}
^{16}O	0.078	Dried food	3.34×10^8	5.55×10^{-16}
		Frozen food	7.65×10^7	1.27×10^{-16}
		Water	2.84×10^7	4.71×10^{-17}
^{56}Fe	0.074	Dried food	3.00×10^7	4.98×10^{-17}
		Frozen food	6.88×10^6	1.14×10^{-17}
		Water	2.55×10^6	4.24×10^{-18}

Table 6: Radiolytic species produced (nMol/L)

Ions at 1 GeV/u	Input parameters			Results				
	D , Gy	Fluence, $1/\mu\text{m}^2$	L , keV/ μm	Concentration of molecules (nMol/L)				
				H.	.OH	H ₂ O ₂	H ₂	e ⁻ _{aq}
P	0.335	9.40	0.22	33.0	188.1	3.7	10.6	146.7
α	0.131	0.919	0.89	12.1	69.3	1.3	3.9	53.9
¹⁶ O	0.078	3.42×10^{-2}	14.24	8.1	46.7	0.9	2.6	36.3
⁵⁶ Fe	0.074	3.07×10^{-3}	150.42	7.4	42.3	0.8	2.4	34.5
Total	0.618	-	-	60.6	346.4	6.7	19.5	271.4

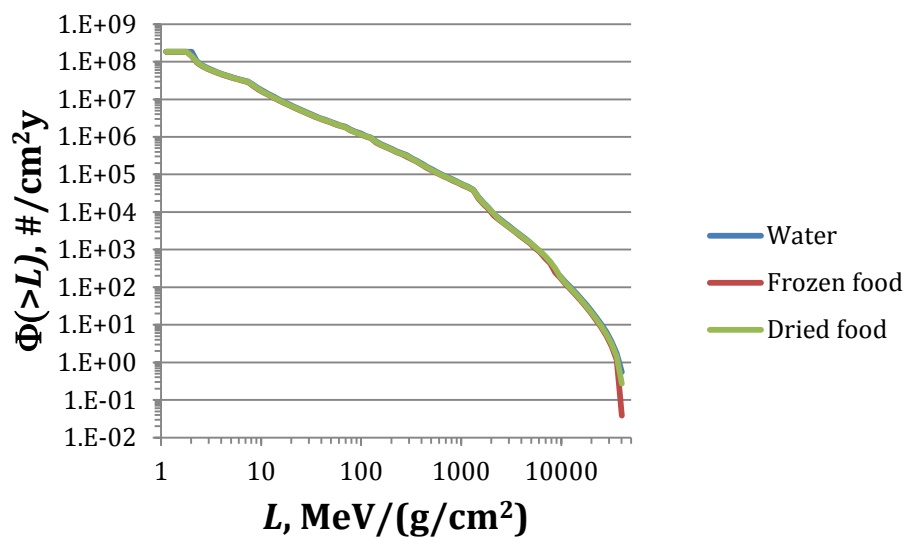


Figure 1a. LET distribution of integral particle fluence inside a Mars transfer vehicle for a 1-y interplanetary space.

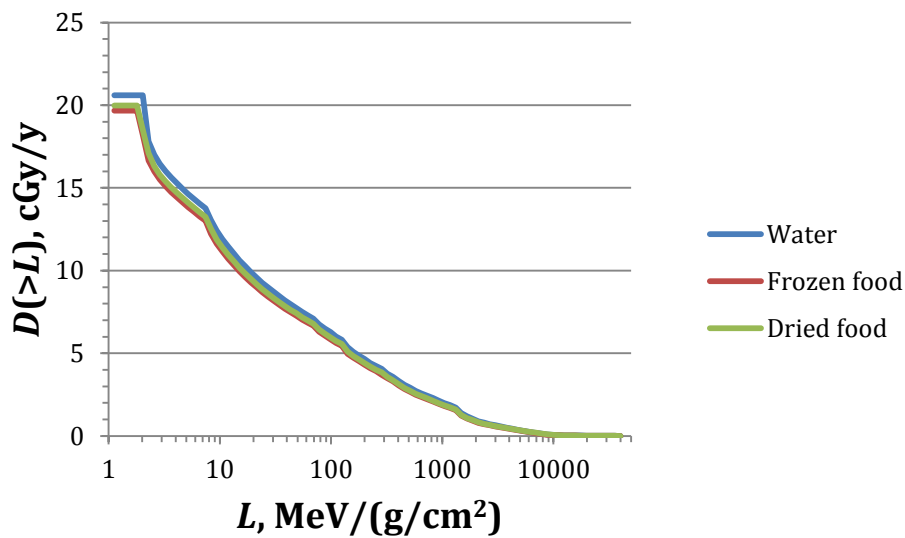


Figure 1b. LET distribution of integral dose inside a Mars transfer vehicle for a 1-y interplanetary space.

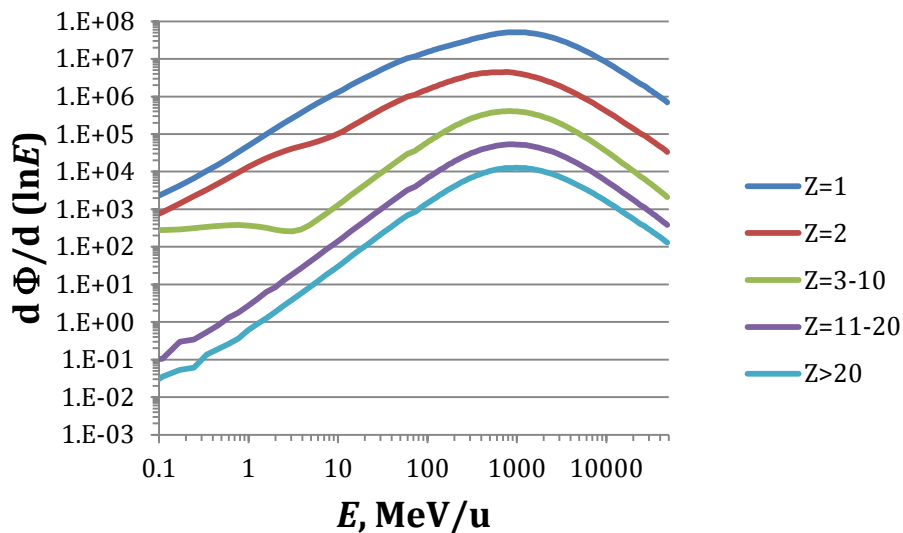


Figure 2a. Differential spectra of annual particle fluence per logarithmic interval of energy per nucleon on water inside a Mars transfer vehicle.

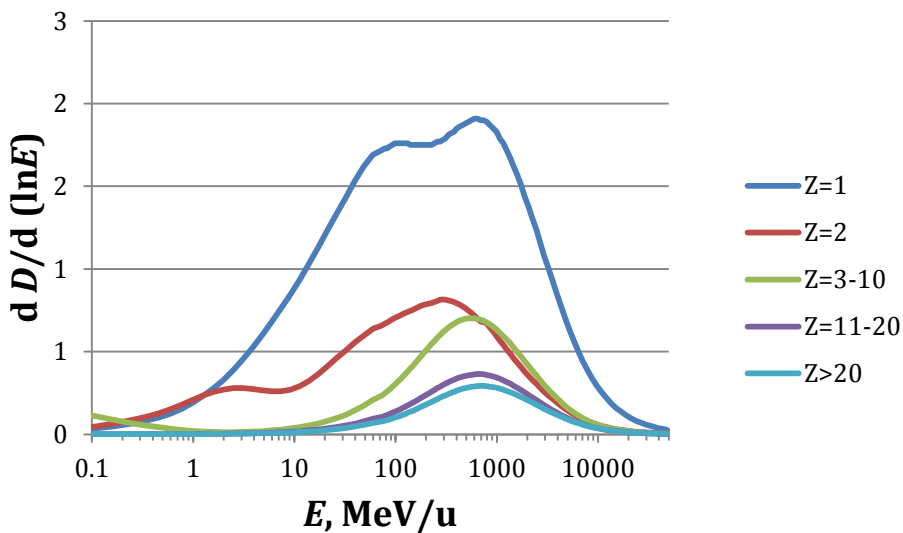


Figure 2b. Differential spectra of annual dose per logarithmic interval of energy per nucleon on water inside a Mars transfer vehicle.

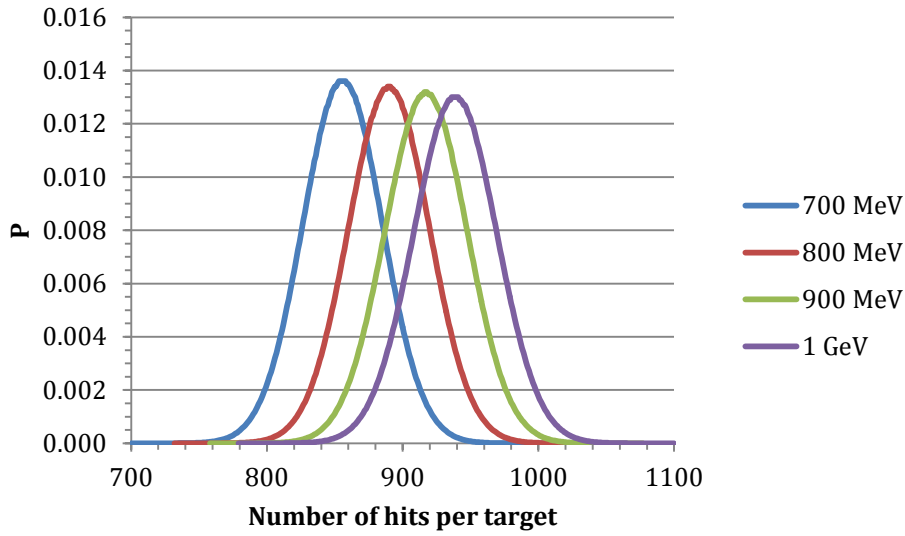


Figure 3. Probability density of number of hits by protons for target area of $100 \mu\text{m}^2$ from exposure to 0.335 Gy of protons at various energies

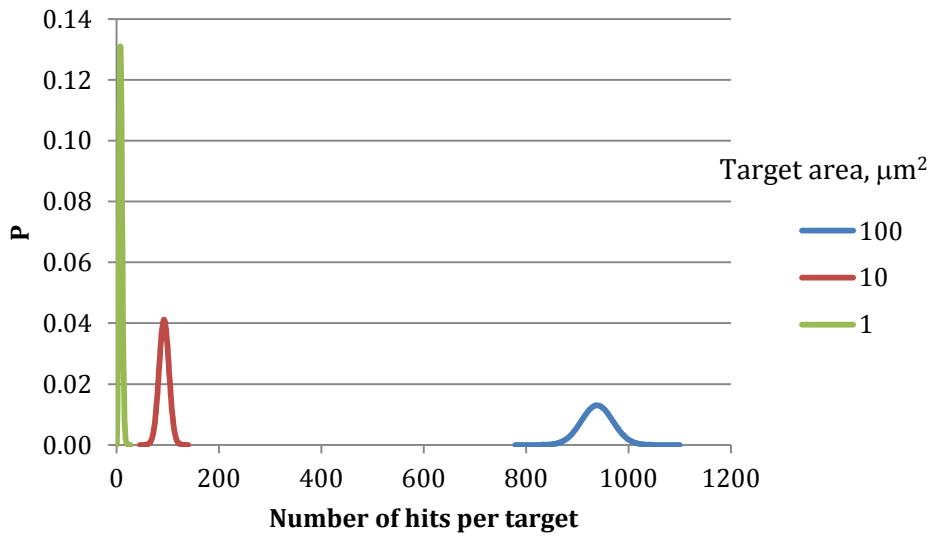


Figure 4. Probability density of number of hits by protons for various target areas from exposure to 0.335 Gy of protons at 1 GeV.